Proceedings of the 9th Workshop on Quantum Chaos and Localisation Phenomena, May 24–26, 2019, Warsaw, Poland

Investigation of the Wigner Reaction Matrix of Microwave Networks Simulating Quantum Graphs with Broken Time Reversal Symmetry-One-Port Investigation

M. Ławniczak, S. Bauch, V. Yunko, M. Białous, J. Wrochna and L. Sirko*
Institute of Physics, Polish Academy of Sciences, Aleja Lotnikow 32/46, PL-02668 Warsaw, Poland

We present new experimental studies of distributions of the Wigner reaction K matrix for open microwave networks. The one-port measurements were performed for the systems with broken time reversal symmetry in the regime of strong losses, where resonances are not resolved. Our studies are complementary to the previous two-port investigations. Fully connected six-vertex microwave networks were used to simulate quantum chaotic systems with broken time reversal symmetry. The usability of the distributions of the Wigner reaction K matrix as an effective tool for evaluation of losses in chaotic systems has been confirmed.

DOI: 10.12693/APhysPolA.136.811
PACS/topics: 05.45.Mt,03.65.Nk

1. Introduction

A description of large complicated quantum systems, for example, nuclear scattering systems, using the Schrödinger equation is very inefficient. In 1959 Wigner successfully proposed to use random matrices for such a purpose [1]. Later, Bohigas et al. showed that some features of quantum chaotic billiards may be described by random matrices [2]. It was with the development of numerical calculations that the highway was opened for theoretical studies of complex quantum systems [3–5]. On the other hand, there is a lack of experimental studies because controllable experimental investigation of such systems is very difficult and sometimes even impossible. Introducing microwave cavities (resonators) [6, 7] and networks [8] simulating respectively quantum billiards and graphs improved this situation. The experiments in the microwave domain are well controlled and are relatively cheap.

Quantum graphs were introduced by Pauling [9]. They are the structures consisting of zero-dimensional vertices connected by one-dimensional bonds and are widely used to model real physical systems whose size in one dimension is much larger than in other dimensions. Among others, they allow to study properties of bounded quantum systems, which are chaotic in the classical limit [8, 10–17] and open systems, which display chaotic scattering [18–21]. The examples of systems and models described by quantum graphs are superconducting quantum circuits [22], quantum circuits in tunnel junctions [23], experimental setups to realize high-dimensional multipartite quantum states [24], discrete-time quantum gravity models [25], and functional connectivity in preclinical Alzheimer's disease [26]. Quantum graphs [10, 11, 13] may be simulated by microwave networks (graphs) [8, 27] consisting of microwave joints (vertices) connected by microwave cables (bonds). This is possible because the Schrödinger equation describing a quantum graph is formally analogous to the telegraph's equation for signal propagation in a microwave network. It should be noticed that only microwave networks provide the experimental simulation of quantum systems representing all three symmetry classes in the random matrix theory (RMT), namely: systems with preserved time reversal symmetry (TRS) belonging to the Gaussian orthogonal ensemble (GOE, $\beta = 1$) [8, 20, 28, 29], or to the Gaussian symplectic ensemble (GSE, $\beta = 4$) [30] and the systems with broken TRS belonging to the Gaussian unitary ensemble (GUE, $\beta = 2$) [8, 18, 31–33]. One should generally mention that the model systems such as microwave networks [8, 27, 28, 32, 34], flat microwave cavities [35–40] and experiments using the Rydberg atoms strongly driven by microwave fields [41–47] appeared to be very successful in simplifying analysis of complex quantum systems.

Properties of TRS invariant open systems ($\beta = 1$) have been extensively studied in many aspects. The statistical distributions of a single-channel scattering matrix S were investigated, taking into account imperfect coupling and direct processes, theoretically [48–53] and experimentally [54]. The distributions of the reflection coefficient $P(R)$ and the imaginary $P(v)$ and the real $P(u)$ parts of the Wigner reaction matrix were theoretically studied in the whole range of the dimensionless parameter $\gamma = 2\pi\Gamma/\Delta$, being a measure of system losses [55, 56], where Γ and Δ are the resonance width and the mean level spacing, respectively. It is worth noting that the imaginary part ($v > 0$) of the Wigner reaction matrix $K \equiv u - \mathrm{i}\,v$ is known in solid-state physics as the local density of states (LDoS) [55]. Experimentally the Wigner reaction matrix K was investigated in microwave cavities [35, 57, 58] and for moderate and

*corresponding author; e-mail: sirko@ifpan.edu.pl

strong losses $\gamma \leq 47.7$ in microwave networks [20, 59–61]. Quantum networks with leads are very interesting open systems and therefore they were also thoroughly studied theoretically [14, 19, 21, 62].

The open chaotic systems with broken TRS ($\beta = 2$) and high losses are much less known. They have been fragmentarily studied experimentally till now. Elastic enhancement factor for microwave networks was measured for the parameter range $7 < \gamma < 62$ [18, 63].

In this paper we present an experimental study of the distributions of the real and imaginary parts of the Wigner reaction matrix K [55, 64, 65] for a fully connected six-vertex [66], irregular network simulating a quantum graph with broken time reversal symmetry. This study complements our previous research, the results of which have been published in [20, 59, 67], on one-channel investigations in the case of strong losses.

2. Theoretical outline

The distribution of the one-channel reaction K matrix can be obtained from the normalized scattering matrix s of a network evaluated for the perfect coupling to the system, when direct processes are not present [53, 58, 68]:

$$K = \mathrm{i}\frac{s-1}{s+1}. \tag{1}$$

The relationship between the matrix s and the scattering matrix S measured directly in the experiment will be discussed in detail later. The reaction matrix K is also related to the network normalized impedance [58] z: $K = -\mathrm{i}z$.

Generally, the scattering matrix S is a square matrix of a dimension equal to the number of ports connected to the scattering system, however in the case of single channel measurements S is just a complex number. It can be parameterized as

$$S = \sqrt{R}\mathrm{e}^{\mathrm{i}\theta}, \tag{2}$$

where R and θ are the reflection coefficient and the phase measured at the port of the network, respectively.

In this study we will analyze the distribution $P(R)$ of the reflection coefficient R and the distributions of the real $P(u)$ and imaginary $P(v)$ parts of the Wigner reaction matrix.

The distribution of the reflection coefficient $P(R)$ is given by [52, 56, 69]:

$$P(R) = \frac{2}{(1-R)^2}P_0\Big(\frac{1+R}{1-R}\Big). \tag{3}$$

The probability distribution $P_0(x)$ for systems with one perfect coupled channel and with broken time reversal symmetry $\beta = 2$ is an analytical expression [52, 56, 69]:

$$P_0(x) = \frac{1}{2}\Big[A\Big(\frac{\alpha(x+1)}{2}\Big)^{\beta/2} + B\Big]\exp\Big(-\frac{\alpha(x+1)}{2}\Big), \tag{4}$$

where $\alpha = \gamma\beta/2$, $A = \mathrm{e}^{\alpha} - 1$, and $B = 1 + \alpha - \mathrm{e}^{\alpha}$.

The distributions of the real $P(u)$ and imaginary $P(v)$ parts of the Wigner reaction matrix are also expressed by the probability distribution $P_0(x)$ [55]:

$$P(u) = \frac{1}{2\pi\sqrt{u^2+1}}\int_0^{\infty}\mathrm{d}q P_0\Big[\frac{\sqrt{u^2+1}}{2}\Big(q+\frac{1}{q}\Big)\Big], \tag{5}$$

and

$$P(v) = \frac{\sqrt{2}}{\pi v^{3/2}}\int_0^{\infty}\mathrm{d}q P_0\Big[q^2+\frac{1}{2}\Big(v+\frac{1}{v}\Big)\Big], \tag{6}$$

where $u = \mathrm{Re}K$ is the real part and $v = -\mathrm{Im}K > 0$ is the imaginary element of K matrix.

In the case of one-channel, perfect coupled systems with preserved time reversal symmetry the probability distribution is defined by its integrated distribution $W(x) = \int_x^{\infty} P_0(x)\mathrm{d}x$ [53, 56]:

$$W(x) = \frac{x+1}{4\pi}\Big[f_1(\omega)g_2(\omega) + f_2(\omega)g_1(\omega) + h_1(\omega)j_2(\omega) + h_2(\omega)j_1(\omega)\Big]_{\omega=\frac{1}{2}(x-1)}, \tag{7}$$

with auxiliary functions f, g, h, j in the following form:

$$\begin{aligned}
f_1(\omega) &= \int_{\omega}^{\infty}\mathrm{d}t\frac{\sqrt{t|t-\omega|}\mathrm{e}^{-\frac{\gamma t}{2}}}{(1+t)^{3/2}}[1-\mathrm{e}^{-\gamma}+t^{-1}],\\
g_1(\omega) &= \int_{\omega}^{\infty}\mathrm{d}t\frac{1}{\sqrt{t|t-\omega|}}\frac{\mathrm{e}^{-\frac{\gamma t}{2}}}{(1+t)^{3/2}},\\
h_1(\omega) &= \int_{\omega}^{\infty}\mathrm{d}t\frac{\sqrt{t|t-\omega|}\mathrm{e}^{-\frac{\gamma t}{2}}}{\sqrt{t(1+t)}}[\gamma+(1-\mathrm{e}^{-\gamma})(\gamma t-2)],\\
j_1(\omega) &= \int_{\omega}^{\infty}\mathrm{d}t\frac{1}{\sqrt{t|t-\omega|}}\frac{\mathrm{e}^{-\frac{\gamma t}{2}}}{\sqrt{1+t}},
\end{aligned} \tag{8}$$

and their counterparts with the index $\beta = 2$ are the same, but with the integration borders $[0, \omega]$ instead of $[\omega, \infty]$.

In both cases, in the limit of large losses, the distribution of reflection coefficient can be approximated by the Rayleigh distribution

$$P(R) = \alpha e^{-\alpha R}, \tag{9}$$

and the formulae (5) and (6) take the forms

$$P(u) = \sqrt{\frac{\alpha}{4\pi}}\exp(-\frac{\alpha u^2}{4}) \tag{10}$$

and

$$P(v) = \sqrt{\frac{\alpha}{4\pi v^3}}\exp\left(-\frac{\alpha}{4}\left(\sqrt{v}-\frac{1}{\sqrt{v}}\right)\right). \tag{11}$$

It should be emphasized that in the case of strong losses due to strong absorption and/or strong coupled channels opening a system, conventional measures of its chaoticity and symmetry class based on spectral correlation functions are useless since overlapping energy levels preclude determining their positions. Then, apart from the Wigner reaction matrix also the elastic enhancement factor [18, 70, 71] can be used for this purpose. However, using it requires 2-port measurements, which is unnecessary for the Wigner reaction matrix.

3. Experiments

To determine the Wigner reaction matrix we measured the scattering matrix S of the 6-vertex (hexagon), fully connected microwave networks, simulating quantum graphs with broken time reversal symmetry ($\beta = 2$). This was verified in the earlier two-port experiment [67] performed for a similar system.

A microwave network contains vertices (microwave joints) connected by bonds (coaxial cables). The six- and five-arm microwave joints were manufactured in our laboratory. The SMA-RG402 coaxial cables with an inner conductor of radius $r_1 = 0.05$ cm and an outer tubular conductor of the inner radius $r_2 = 0.15$ cm were applied. The conductors are insulated by Teflon with a dielectric constant $\varepsilon \simeq 2.06$ [72, 73] that fills the space between them. Only the fundamental TEM mode can propagate in the coaxial cables below the onset frequency of the next TE_{11} mode. This cut-off frequency is $\nu_{\rm cut} \simeq \frac{c}{\pi(r_1+r_2)\sqrt{\varepsilon}} \simeq 33$ GHz [74], where c is the speed of light in vacuum. Absorption of the networks can be controlled by changing their length and/or by introducing to them microwave attenuators [59, 60]. In these measurements fifteen 2 dB attenuators, one at each bond, were introduced. The experimental setup is shown in Fig. 1.

To simulate the quantum graphs with broken TRS four Anritsu PE8403 microwave circulators with low insertion loss which operate in the frequency range 7–14 GHz were introduced to the networks. These are non-reciprocal three-port passive devices. A wave entering the circulator through port 1, 2, or 3 goes out through the port 2, 3, or 1, respectively (see Fig. 1).

Different networks realizations were created primarily with the help of four phase shifters (see Fig. 1). In one step, the optical lengths of each of the two selected bonds were changed by 0.5 cm by a corresponding pair of phase shifters giving a change in the total length of the network by 1 cm. Then the same was repeated for the second pair of bonds. Finally, after 20 such steps the total optical length was changed by 20 cm. Next, one of the network bond was replaced with a longer one and the procedure with the phase shifters was repeated. In this way 127 realizations of the network simulating a GUE system with the total optical length between 7.78 and 9.12 m were obtained.

A vector network analyzer (VNA) Agilent E8364B was used to measure the scattering matrix S. The network was connected to VNA via the lead — HP 85133-616 flexible microwave cable attached to the only six-arm vertex of it. The measurements were carried out in the frequency range 7–14 GHz corresponding to the operation range of the circulators. The example of the observed spectrum in the frequency range 10–11 GHz is shown in Fig. 2.

In order to obtain elements of the Wigner reaction matrix and the mean reflection coefficient $\langle R\rangle = \langle ss^\dagger\rangle$ from the experimentally measured scattering matrix S, it is necessary to extract its s value for a perfect coupling

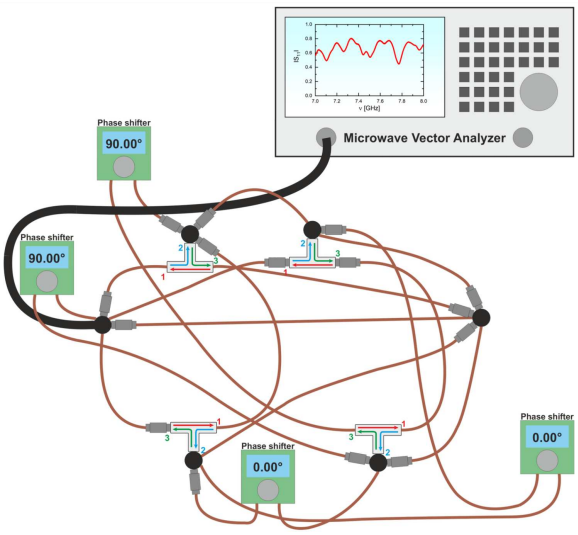

Fig. 1. The experimental setup for the measurements of the one-port scattering matrix S. Six-vertex, fully connected network, consisting of 15 bonds and attenuators, four circulators and four phase shifters is connected to the vector network analyzer Agilent E8364B via 85133-616 flexible microwave cable.

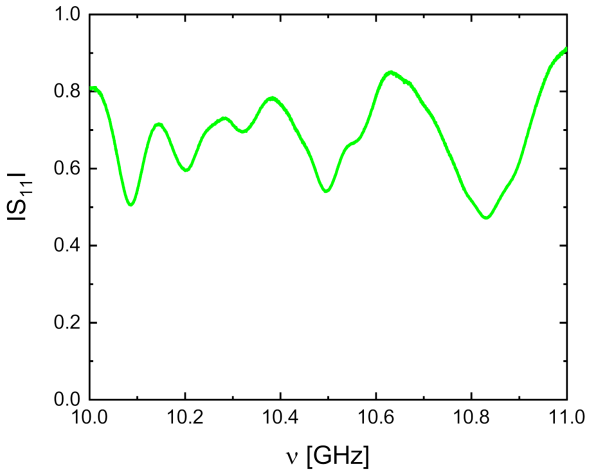

Fig. 2. An example of the measured modulus $|S|$ of the one-port scattering matrix S in the frequency range 10–11 GHz. The measurements were done for the network containing 2 dB attenuators yielding $\gamma = 46.2 \pm 5.1$. Since γ is large, all resonances are overlapping.

by eliminating direct processes. It should be noted that in the case of quantum graphs and simulating them microwave networks with the Neumann boundary conditions the perfect coupling with outside world is even theoretically impossible. This is the result of a non zero probability of the input signal reflection (back scattering) ($|\sigma^i_j|^2$) at any non-trivial vertex i of a valency $v_i \geq 3$ [11]. The valency of a vertex is the number of edges connected to it for quantum graphs

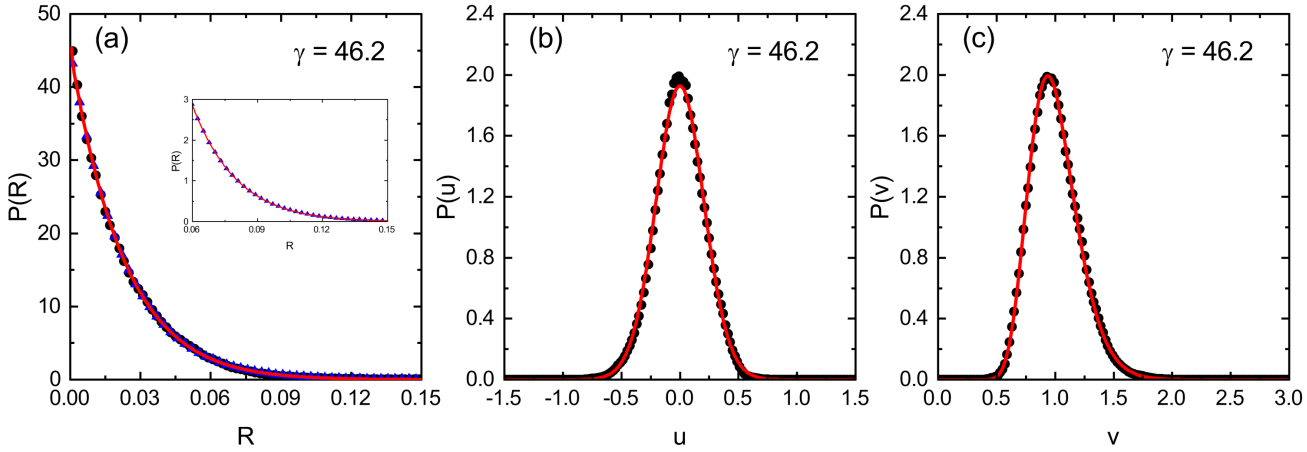

Fig. 3. The distributions of reflection coefficient $P(R)$, the real $P(u)$ and imaginary $P(v)$ parts of Wigner reaction matrix for the one-port measurements. The full circles mark experimental data while the solid lines represent theoretical predictions for systems with one strongly coupled channel. The theoretical distribution of the reflection coefficient $P(R)$ approximated by the Rayleigh formula (9) is marked by triangles in part (a). The application of this formula yielded $\gamma = 46.1 \pm 5.2$. The inset in part (a) shows the comparison of the theoretical distributions of the reflection coefficient $P(R)$ calculated from the accurate formula (3) (solid line) and the Rayleigh formula (9) (triangles).

and the number of arms of the microwave joint in the case of microwave networks. This probability increases with number of connections (arms) of the vertex

$$|\sigma_j^i|^2 = \left| -\delta_{ij} + \frac{2}{v_i} \right|^2 . \tag{12}$$

The elimination of direct processes can be done using the Poison kernel, the distribution of a phase of a scattering matrix [53, 54, 59] or in case of microwave systems also with the help of impedance approach [35, 58], in which electrical properties of the system are exploited. The normalized scattering matrix without direct processes s is related to the normalized impedance z, as follows:

$$s = \frac{1-z}{1+z}, \tag{13}$$

where the normalized impedance z of a chaotic microwave network is given by

$$z = (\mathrm{Re}Z^r)^{-1/2}[\mathrm{Re}Z + \mathrm{i}(\mathrm{Im}Z - \mathrm{Im}Z^r)](\mathrm{Re}Z^r)^{-1/2}. \tag{14}$$

In this formula $Z = Z_0^{1/2}(1+S)/(1-S)Z_0^{1/2}$ and $Z^r = Z_0^{1/2}(1+S^r)/(1-S^r)Z_0^{1/2}$ are the network and the radiation impedance matrices expressed, respectively, by the network S and the radiation S^r scattering matrices. Z_0 is a characteristic impedance of the network bonds attached to the 6-arm joint. The radiation scattering matrix S^r was measured at the input of the 6-arm vertex. When the number of external leads attached to the vertex is smaller than the number of internal edges attached to it, we call this vertex unbalanced [34]. Such vertices are used, e.g., in the recent photovoltaic smartwire connection technology [75]. The remaining 5 vertex arms were closed with 50 Ω loads simulating its infinity shift.

The parameter γ of the system was evaluated by fitting the theoretical mean reflection coefficient

$$\langle R \rangle^{th} = \int_0^1 \mathrm{d}R\, R\, P(R) \tag{15}$$

to the experimental one $\langle R \rangle = \langle ss^\dagger \rangle$ obtained after eliminating the direct processes.

The review of Eqs. (9)–(11) shows that the distributions $P(R)$, $P(u)$, and $P(v)$ will be formally the same for the GUE and GOE systems, if instead of γ, $\gamma/2$ will be introduced for GOE system. This feature can be used to distinguish the symmetry of the system under study, if it is possible to perform an independent evaluation of the parameter γ.

4. Results

The obtained distributions of the reflection coefficient $P(R)$, the real $P(u)$ and imaginary $P(v)$ parts of the Wigner reaction matrix from the one-port measurements are presented in Fig. 3 in part (a), (b), and part (c), respectively. The full circles denote experimental values, while the solid line represents the theoretical curves fitted to the experimental results by finding the proper value of the parameter γ. The theoretical curves were calculated from the formulae (3), (5), and (6). The agreement between the experimental data and the theoretical predictions is very good. Only for the real part $P(u)$ of the Wigner reaction matrix some visible discrepancies appeared. It is clearly seen that the decay of the reflection coefficient $P(R)$ is given by a single exponential function, as expected from the formula (9).

The value of γ evaluated by fitting the theoretical mean reflection coefficient to the experimental results $\langle R \rangle = \langle ss^\dagger \rangle$ obtained after eliminating the direct processes (see formulae (13)–(15)) is 46.2 ± 5.1. The application of the Rayleigh formula (9) yielded $\gamma = 46.1 \pm 5.2$.

The theoretical distribution of the reflection coefficient $P(R)$ given by formula (9) is marked by triangles in Fig. 3a. The inset in panel (a) shows the comparison of the theoretical distributions of the reflection coefficient $P(R)$ calculated from the accurate formula (3) (solid line) and the Rayleigh formula (9) (triangles). As we can see, both results are very close to each other even in the tails of the distributions. The statement that in the limit of strong losses the distribution of the reflection coefficient $P(R)$ can be approximated by a simple exponential function (formula (9)) has been already formulated in [67] in the case of two open channels. Our results confirm the usability of the distributions of the Wigner reaction K matrix as a powerful tool for the evaluation of losses in GUE chaotic systems.

5. Conclusions

We have confirmed that the distributions of the real $P(u)$ and the imaginary $P(v)$ parts of the Wigner reaction matrix are excellent tools for investigating quantum chaotic systems with broken time reversal symmetry, especially, within the limit of strong losses. In such a limit due to overlapping of energy levels it is extremely difficult or even impossible to apply the conventional measures of chaoticity of quantum systems such as the spectral correlation functions. In the limit of strong losses the use of the distributions of the real $P(u)$ and the imaginary $P(v)$ parts of the Wigner reaction matrix supplements the application of the elastic enhancement factor in more versatile characterization of chaotic systems.

Acknowledgments

This work was supported in part by the National Science Centre, Poland, Grant No. UMO-2018/30/Q /ST2/00324 and the National Centre for Research and Development, Grant POIR.04.01.04-00-0144/17.

References

[1] E.P. Wigner, *Ann. Math.* **62**, 548 (1959).

[2] O. Bohigas, M.J. Giannoni, C. Schmit, *Phys. Rev. Lett.* **52**, 1 (1984).

[3] H.J. Stöckmann, *Quantum Chaos: An Introduction*, Cambridge University Press, Cambridge 2000.

[4] F. Haake, *Quantum Signatures of Chaos*, Springer-Verlag, Heidelberg 2001.

[5] H.A. Weidenmüller, G.E. Mitchell, *Rev. Mod. Phys.* **81**, 539 (2009).

[6] H.J. Stöckmann, J. Stein, *Phys. Rev. Lett.* **64**, 2215 (1990).

[7] E. Doron, U. Smilansky, *Phys. Rev. Lett.* **65**, 3072 (1990).

[8] O. Hul, Sz. Bauch, P. Pakoński, N. Savytskyy, K. Życzkowski, L. Sirko, *Phys. Rev. E* **69**, 056205 (2004).

[9] L.J. Pauling, *Chem. Phys.* **4**, 673 (1936).

[10] T. Kottos, U. Smilansky, *Phys. Rev. Lett.* **79**, 4794 (1997).

[11] T. Kottos, U. Smilansky, *Ann. Phys.* **274**, 76 (1999).

[12] G. Tanner, *J. Phys. A* **33**, 3567 (2000).

[13] F. Barra, P. Gaspard, *J. Stat. Phys.* **101**, 283 (2000).

[14] T. Kottos, H. Schanz, *Physica E* **9**, 523 (2001).

[15] P. Pakoński, K. Życzkowski, M. Kuś, *J. Phys. A* **34**, 9303 (2001).

[16] R. Blümel, Yu. Dabaghian, R.V. Jensen, *Phys. Rev. Lett.* **88**, 044101 (2002).

[17] P. Pakoński, G. Tanner, K. Życzkowski, *J. Stat. Phys.* **111**, 1331 (2003).

[18] M. Ławniczak, S. Bauch, O. Hul, L. Sirko, *Phys. Rev. E* **81**, 046204 (2010).

[19] T. Kottos, U. Smilansky, *Phys. Rev. Lett.* **85**, 968 (2000).

[20] M. Ławniczak, O. Hul, S. Bauch, P. Šeba, L. Sirko, *Phys. Rev. E* **77**, 056210 (2008).

[21] Z. Pluhař, H.A. Weidenmüller, *Phys. Rev. Lett.* **112**, 144102 (2014).

[22] H.Z. Jooya, K. Reihani, S.I. Chu, *Sci. Rep.* **6**, 37544 (2016).

[23] O.F. Namarvar, G. Dridi, C. Joachim, *Sci. Rep.* **6**, 30198 (2016).

[24] M. Krenn, X. Gu, A. Zeilinger, *Phys. Rev. Lett.* **119**, 240403 (2017).

[25] P. Arrighi, S. Martiel, *Phys. Rev. D* **96**, 024026 (2017).

[26] M.R. Brier, J.B. Thomas, A.M. Fagan, J. Hassenstab, D.M. Holtzman, T.L. Benzinger, J.C. Morris, B.M. Ances, *Neurobiol. Aging* **35**, 757 (2014).

[27] M. Ławniczak, S. Bauch, L. Sirko, in: *Handbook of Applications of Chaos Theory*, Eds. C.H. Skiadas, C. Skiadas, CRC Press, Boca Raton 2016, p. 559.

[28] O. Hul, M. Ławniczak, Sz. Bauch, A. Sawicki, M. Kuś, L. Sirko, *Phys. Rev. Lett.* **109**, 040402 (2012).

[29] B. Dietz, V. Yunko, M. Białous, Sz. Bauch, M. Ławniczak, L. Sirko, *Phys. Rev. E* **95**, 052202 (2017).

[30] A. Rehemanjiang, M. Allgaier, C.H. Joyner, S. Müller, M. Sieber, U. Kuhl, H.J. Stöckmann, *Phys. Rev. Lett.* **117**, 064101 (2016).

[31] M. Allgaier, S. Gehler, S. Barkhofen, H.-J. Stöckmann, U. Kuhl, *Phys. Rev. E* **89**, 022925 (2014).

[32] M. Białous, V. Yunko, Sz. Bauch, M. Lawniczak, B. Dietz, L. Sirko, *Phys. Rev. Lett.* **117**, 144101 (2016).

[33] M. Ławniczak, M. Białous, S. Bauch, B. Dietz, L. Sirko, *Acta Phys. Pol. A* **132**, 1672 (2017).

[34] M. Ławniczak, J. Lipovský, L. Sirko, *Phys. Rev. Lett.* **122**, 140503 (2019).

[35] S. Hemmady, X. Zheng, E. Ott, T.M. Antonsen, S.M. Anlage, *Phys. Rev. Lett.* **94**, 014102 (2005).

[36] L. Sirko, P.M. Koch, R. Blümel, *Phys. Rev. Lett.* **78**, 2940 (1997).

[37] Y. Hlushchuk, A. Błędowski, N. Savytskyy, L. Sirko, *Phys. Scr.* **64**, 192 (2001).

[38] R. Blümel, P.M. Koch, L. Sirko, *Found. Phys.* **31**, 269 (2001).

[39] B. Dietz, A. Richter, *Chaos* **25**, 097601 (2015).

[40] M. Białous, B. Dietz, L. Sirko, *Phys. Rev. E* **100**, 012210 (2019).

[41] R. Blümel, A. Buchleitner, R. Graham, L. Sirko, U. Smilansky, H. Walther, *Phys. Rev. A* **44**, 4521 (1991).

[42] M. Bellermann, T. Bergemann, A. Haffmann, P.M. Koch, L. Sirko, *Phys. Rev. A* **46**, 5836 (1992).

[43] L. Sirko, S. Yoakum, A. Haffmans, P.M. Koch, *Phys. Rev. A* **47**, R782 (1993).

[44] L. Sirko, P.M. Koch, *Appl. Phys. B* **60**, S195 (1995).

[45] L. Sirko, A. Haffmans, M.R.W. Bellermann, P.M. Koch, *Europhys. Lett.* **33**, 181 (1996).

[46] L. Sirko, S.A. Zelazny, P.M. Koch, *Phys. Rev. Lett.* **87**, 043002 (2001).

[47] L. Sirko, P.M. Koch, *Phys. Rev. Lett.* **89**, 274101 (2002).

[48] G. López, P.A. Mello, T.H. Seligman, *Z. Phys. A* **302**, 351 (1981).

[49] E. Doron, U. Smilansky, *Nucl. Phys. A* **545**, 455 (1992).

[50] P.W. Brouwer, *Phys. Rev. B* **51**, 16878 (1995).

[51] D.V. Savin, Y.V. Fyodorov, H.J. Sommers, *Phys. Rev. E* **63**, 035202 (2001).

[52] Y.V. Fyodorov, *JETP Lett.* **78**, 250 (2003).

[53] Y.V. Fyodorov, D.V. Savin, H.J. Sommers, *J. Phys. A* **38**, 10731 (2005).

[54] U. Kuhl, M. Martinez-Mares, R.A. Méndez-Sánchez, H.J. Stöckmann, *Phys. Rev. Lett.* **94**, 144101 (2005).

[55] Y.V. Fyodorov, D.V. Savin, *JETP Lett.* **80**, 725 (2004).

[56] D.V. Savin, H.J. Sommers, Y.V. Fyodorov, *JETP Lett.* **82**, 544 (2005).

[57] R.A. Méndez-Sánchez, U. Kuhl, M. Barth, C.V. Lewenkopf, H.J. Stöckmann, *Phys. Rev. Lett.* **91**, 174102 (2003).

[58] S. Hemmady, X. Zheng, T.M. Antonsen Jr., E. Ott, S.M. Anlage, *Phys. Rev. E* **74**, 036213 (2006).

[59] O. Hul, O. Tymoshchuk, S. Bauch, P.M. Koch, L. Sirko, *J. Phys. A* **38**, 10489 (2005).

[60] O. Hul, S. Bauch, M. Ławniczak, L. Sirko, *Acta Phys. Pol. A* **112**, 655 (2007).

[61] M. Ławniczak, S. Bauch, O. Hul, L. Sirko, *Phys. Scr.* **T135**, 014050 (2009).

[62] P. Exner, J. Lipovský, *Phys. Lett. A* **375**, 805 (2011).

[63] M. Ławniczak, S. Bauch, O. Hul, L. Sirko, *Phys. Scr.* **T143**, 014014 (2011).

[64] G. Akguc, L.E. Reichl, *Phys. Rev. E* **64**, 056221 (2001).

[65] V.V. Sokolov, O.V. Zhirov, *Phys. Rev. E* **91**, 052917 (2015).

[66] O. Hul, P. Šeba, L. Sirko, *Phys. Rev. E* **79**, 066204 (2009).

[67] M. Ławniczak, L. Sirko, *Sci. Rep.* **9**, 5630 (2019).

[68] M. Ławniczak, S. Bauch, O. Hul, L. Sirko, *Phys. Scr.* **T147**, 014018 (2012).

[69] C.W.J. Beenakker, P.W. Brouwer, *Physica E* **9**, 463 (2001).

[70] M. Ławniczak, M. Białous, V. Yunko, S. Bauch, L. Sirko, *Phys. Rev. E* **91**, 032925 (2015).

[71] M. Ławniczak, M. Białous, V. Yunko, S. Bauch, L. Sirko, *Acta Phys. Pol. A* **128**, 974 (2015).

[72] K.H. Breeden, A.P. Sheppard, *Radio Sci.* **3**, 205 (1968).

[73] N. Savytskyy, A. Kohler, S. Bauch, R. Blümel, L. Sirko, *Phys. Rev. E* **64**, 036211 (2001).

[74] D.S. Jones, *Theory of Electromagnetism*, Pergamon Press, Oxford 1964, p. 254.

[75] T. Söderström, P. Papet, Y. Yao, J. Ufheil, *Smartwire connection technology*, Meyer Burger, 2014.